

## SUPPLEMENTARY INFORMATION

### **A homodimer interface without base pairs in an RNA mimic of red fluorescent protein**

Katherine Deigan Warner<sup>1</sup>, Ljiljana Sjekloća<sup>1</sup>, Wenjiao Song<sup>2</sup>, Grigory S. Filonov<sup>2</sup>, Samie R. Jaffrey<sup>2</sup> & Adrian R. Ferré-D'Amaré<sup>1\*</sup>

<sup>1</sup>Biochemistry and Biophysics Center, National Heart, Lung and Blood Institute, Bethesda, Maryland, USA.

<sup>2</sup>Department of Pharmacology, Weill-Cornell Medical College, Cornell University, New York, New York, USA.

(\* ) Address correspondence to this author. E: [adrian.ferre@nih.gov](mailto:adrian.ferre@nih.gov)

T: 301-496-4096, F: 301-451-5459

## SUPPLEMENTARY RESULTS

**Supplementary Table 1** Crystallographic Statistics

	Crystal I	Crystal II
<b>Data collection</b>		
Space group	$P2_12_12_1$	$P2_12_12_1$
Cell dimensions		
<i>a, b, c</i> (Å)	36.3, 55.3, 99.0	36.6, 55.4, 98.7
Resolution (Å)	50.0 – 2.35 (2.39 – 2.35) <sup>a</sup>	50.0 – 2.50 (2.54 – 2.50)
$R_{\text{merge}}$	0.119 (> 1.0)	0.130 (> 1.0)
$\langle I \rangle / \langle \sigma(I) \rangle$	32.1 (1.2)	23.7 (1.1)
Completeness (%)	99.1 (93.1)	98.8 (88.9)
Redundancy	11.3 (4.2)	12.6 (7.3)
<b>Refinement</b>		
Resolution (Å)	50.0 – 2.35 (2.41 – 2.35)	50.0 – 2.50 (2.58 – 2.50)
No. reflections	7797 (516)	6468 (420)
$R_{\text{work}} / R_{\text{free}}$ (%)	18.0 / 22.8 (30.7 / 41.2)	19.1 / 23.9 (35.8 / 36.7)
No. atoms	1646	1609
RNA	1566	1564
Chromophore	20	20
Buffer/ion	8	12
Water	52	13
$\langle B\text{-factors} \rangle$ (Å <sup>2</sup> )	55.7	45.7
RNA	56.1	45.9
Chromophore	38.1	26.4
Buffer/ion	52.3	65.3
Water	50.2	35.7
R.m.s deviations		
Bond lengths (Å)	0.007	0.008
Bond angles (°)	2.07	1.88

<sup>a</sup>Values in parentheses are for highest-resolution shell. One crystal was used for each data set.

**Supplementary Table 2** Analytical Ultracentrifugation

Sample	frictional ratio	MW of majority peak (Da)	majority peak, % of total
Corn (OD ~ 1)	1.551	28629	90.8
Corn (OD ~ 0.4)	1.558	28891	94.7
Corn (OD ~ 0.05)	1.614	29298	96.9
tRNA <sup>Lys3</sup> (OD ~ 0.6)	1.570	26360	89.7

**Supplementary Table 3** SAXS Analysis

	$R_g$ ( $\pm 0.2$ Å)	$I_0$ ( $\pm 0.07 \times 10^{-2}$ )	$D_{\max}$ ( $\pm 5$ Å)	Porod volume
apo*	20.8	$8.50 \times 10^{-2}$	65	18536
+DFHO*	21.2	$9.16 \times 10^{-2}$	65	18458

\* Data-sets were collected in a single day.

**Supplementary Table 4** Precision for "Split Corn" fluorescence measurements. Each cell indicates the standard error from three independent experiments for the measurements in **Fig. 5a**.

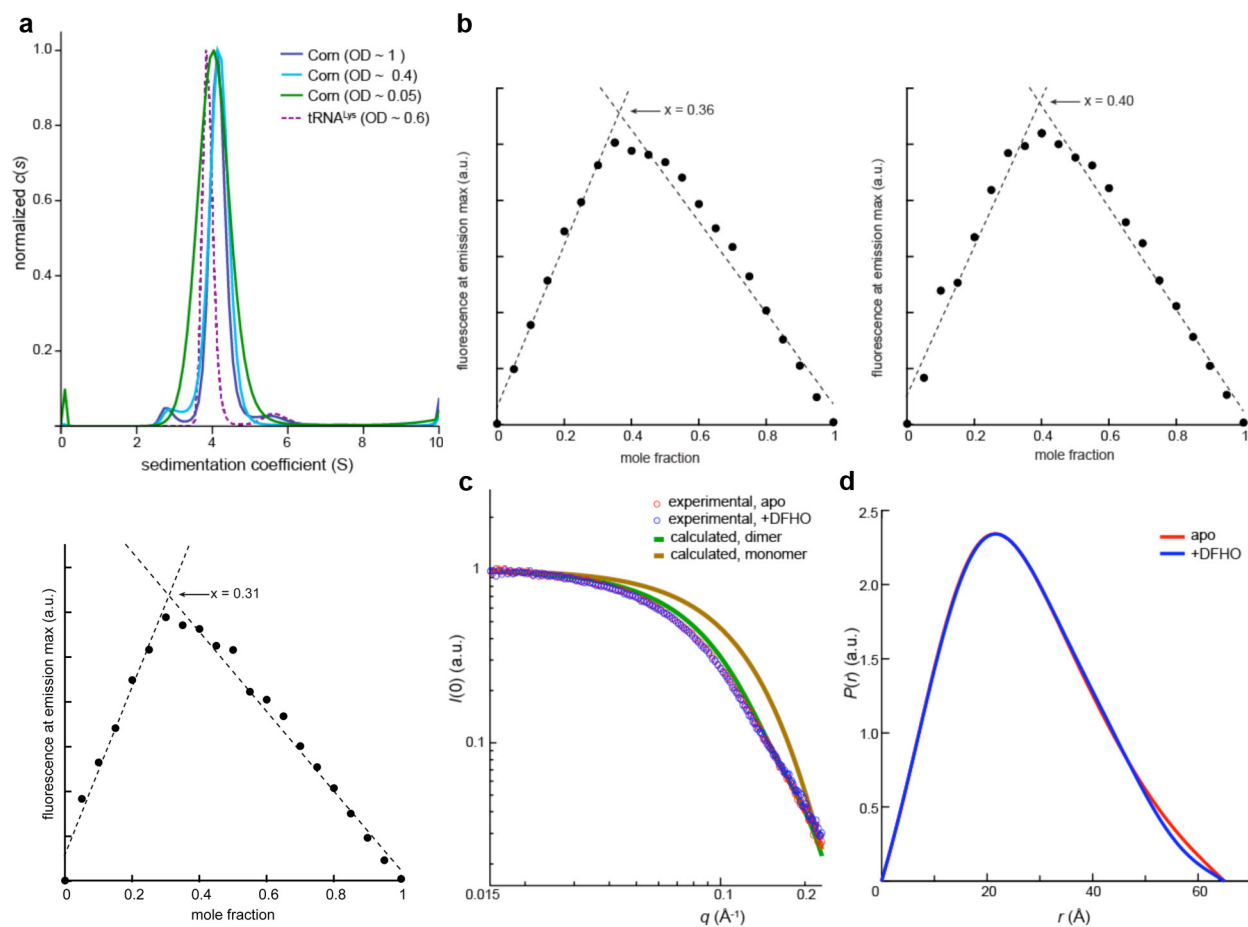
<b>11G</b>	0.013								
<b>11C</b>	0.015	0.010							
<b>11U</b>	0.004	0.021	0.011						
<b>14G</b>	0.005	0.001	0.026	0.002					
<b>14C</b>	0.008	0.004	0.006	0.007	0.005				
<b>14U</b>	0.006	0.006	0.007	0.002	0.005	0.001			
<b>24G</b>	0.012	0.003	0.007	0.018	0.030	0.004	0.001		
<b>24C</b>	0.023	0.011	0.012	0.024	0.038	0.004	0.005	0.002	
<b>24U</b>	0.022	0.006	0.023	0.012	0.017	0.001	0.004	0.004	0.002
<b>11G</b>	<b>11C</b>	<b>11U</b>	<b>14G</b>	<b>14C</b>	<b>14U</b>	<b>24G</b>	<b>24C</b>	<b>24U</b>	

**Supplementary Table 5** Sequences of RNAs used in this study

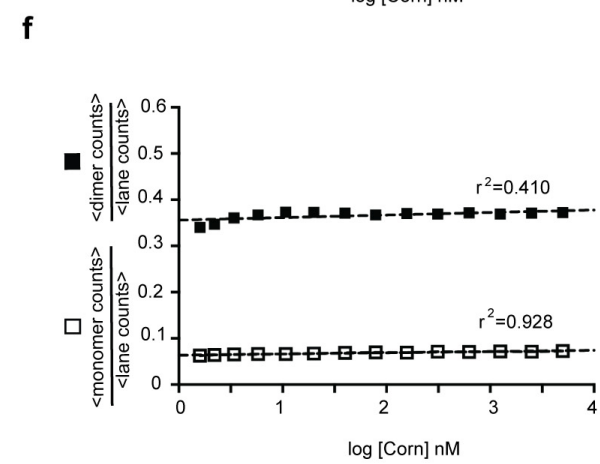
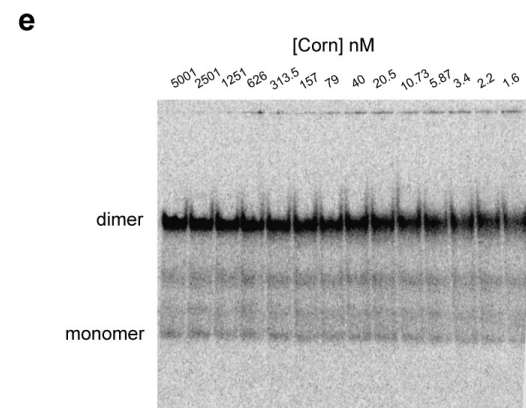
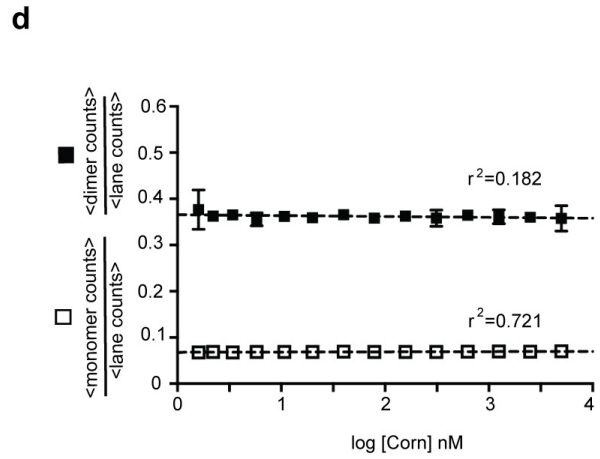
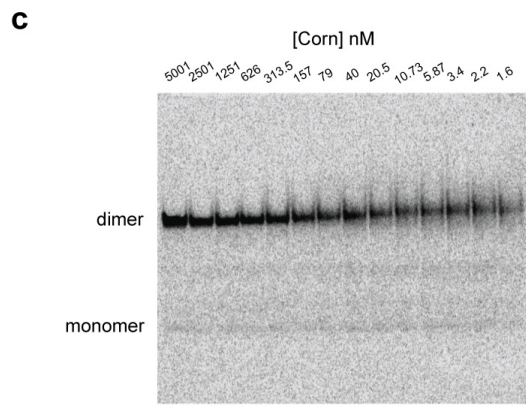
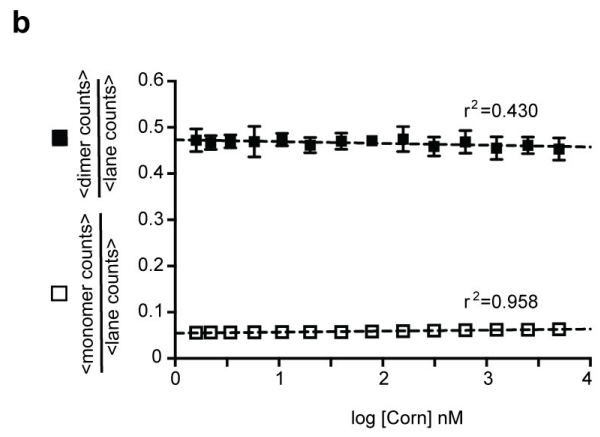
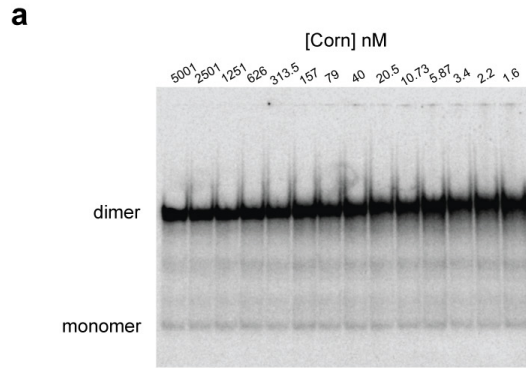
RNA number	RNA name	Sequence (5' – 3')
1	Crystallization construct, 5iodoU	GGCGCGAGGAAGGAGG(U[5I])CUGAGGAGGUCACUGCGCC
2	Crystallization construct, native	GGCGCGAGGAAGGAGGUCUGAGGAGGUCACUGCGCC
3	Native, txn	GGCGCGAGGAAGGAGGUCUGAGGAGGUCACUGCGCC
4	11G	GGCGCGAGGAGGGAGGUCUGAGGAGGUCACUGCGCC
5	11C	GGCGCGAGGACGGAGGUCUGAGGAGGUCACUGCGCC
6	11U	GGCGCGAGGAUGGAGGUCUGAGGAGGUCACUGCGCC
7	14G	GGCGCGAGGAAGGGGGUCUGAGGAGGUCACUGCGCC
8	14C	GGCGCGAGGAAGGCCGGUCUGAGGAGGUCACUGCGCC
9	14U	GGCGCGAGGAAGGUGGUCUGAGGAGGUCACUGCGCC
10	24G	GGCGCGAGGAAGGAGGUCUGAGGGGGUCACUGCGCC
11	24C	GGCGCGAGGAAGGAGGUCUGAGGCCGGUCACUGCGCC
12	24U	GGCGCGAGGAAGGAGGUCUGAGGUGGUCACUGCGCC
13	Baby Spinach	GGUGAAGGACGGGUCCAGUAGUUCGCUACUGUUGAGUAGA GUGUGAGCUCC



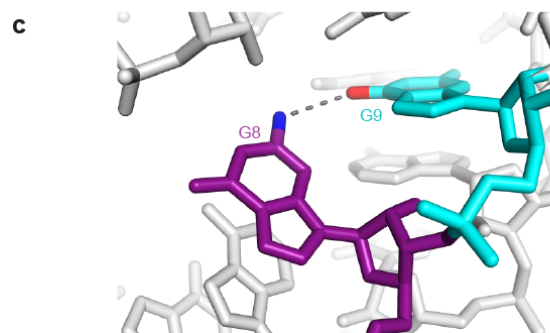
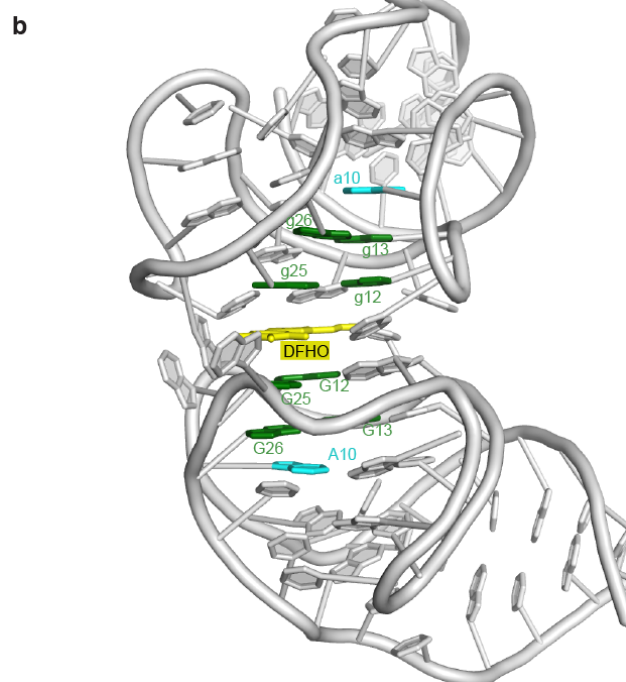
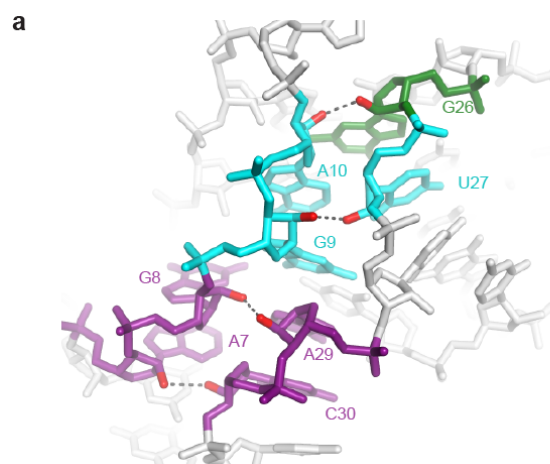
**Supplementary Figure 1** (a) Secondary structure proposed<sup>1</sup> for Corn RNA on the basis of sequence and deletion analyses, color-coded according to **Fig. 1**. The conserved core extends to the two loop-proximal Watson-Crick base pairs of the double-helical portion shown in this schematic. (b) Unbiased, 2.5-resolution density-modified SAD electron density map (contoured at 1.5 s.d. above mean peak height, blue mesh) corresponding to approximately one crystallographic asymmetric unit, oriented as in **Fig. 1d**. The nine-tiered quadruplex-DFHO-quaruplex stack is prominently visible on the left. (c) Unbiased, 2.5 Å resolution density-modified SAD electron density map (contoured at 1.5 s.d. above mean peak height, blue mesh) corresponding to the region around the bound DFHO molecule, looking down on protomer A, superimposed on the refined crystallographic model. (d) Unbiased, 2.5 Å resolution density-modified SAD electron density map (contoured at 1.5 s.d. above mean peak height, blue mesh) corresponding to the region around the bound DFHO molecule, looking down on protomer B, superimposed on the refined crystallographic model. (e) Stereoview of a cartoon representation of the Corn dimer structure, shown as in **Fig. 1d**.



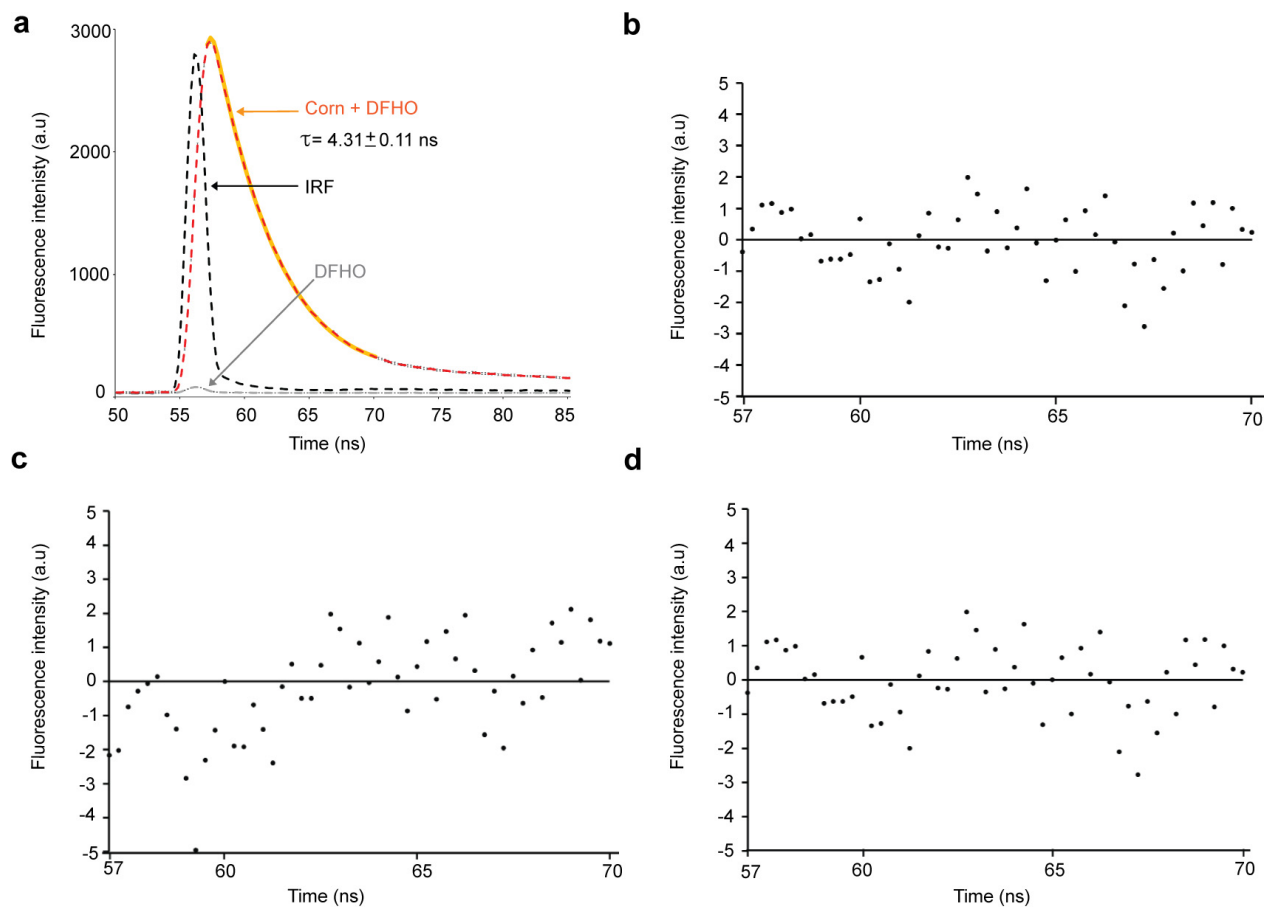
**Supplementary Figure 2** Biophysical analyses supporting a 1:2 DFHO:RNA stoichiometry in solution. **(a)** Normalized  $c(s)$  distributions for Corn RNA at three concentrations, and tRNA<sup>Lys3</sup> at a single concentration. **(b)** Three replicate Job plot analyses of Corn:DFHO stoichiometry, the average of which is shown in **Fig. 2c**. **(c)** Comparison of the scattering profile back-calculated from the model of DFHO-bound Corn (Crystal I, "dimer") and one RNA chain of DFHO-bound Corn (Crystal I, "monomer") and the experimental solution X-ray scattering of DFHO-bound and free Corn RNA (RNA 3, **Supplementary Table 5**). **(d)**  $P(r)$  (distance distribution) function for free and DFHO-bound Corn RNA.



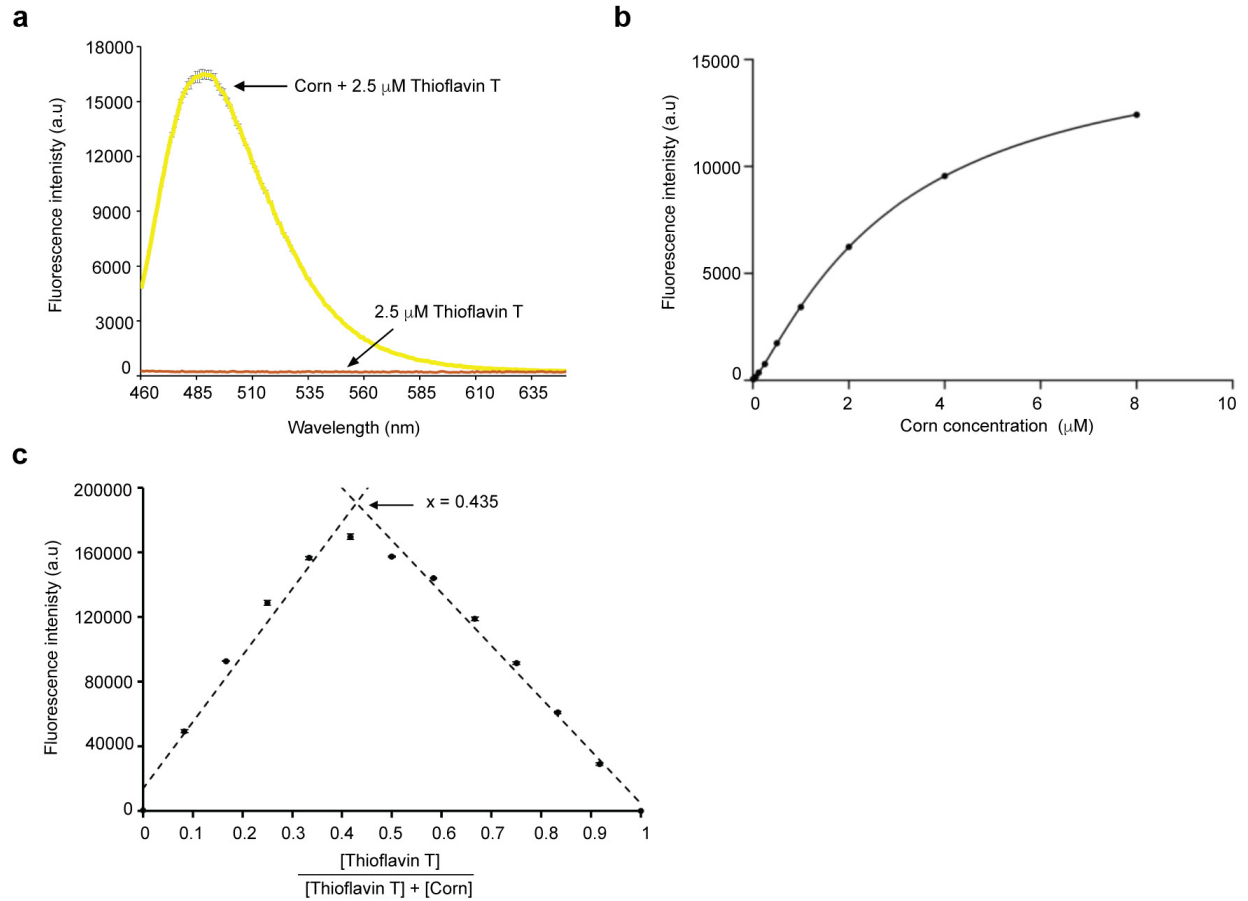
**Supplementary Figure 3** Non-denaturing electrophoretic analyses of serial dilutions of Corn in the absence of DFHO. Radiolabeled Corn RNA (15 fmol, ~ 100 cpm) was diluted with unlabeled Corn RNA to yield total RNA concentrations of 5  $\mu$ M, 2.5  $\mu$ M, 1.25  $\mu$ M, 630 nM, 314 nM, 157 nM, 80 nM, 40 nM, 21 nM, 10.7 nM, 5.9 nM, 3.4 nM, 2.2 nM and 1.6 nM (on a monomer basis). After incubation in 90  $\mu$ g ml<sup>-1</sup> BSA, 5% (w/v) PEG 8000, 50 mM HEPES-KOH pH 7.5, 0.1 M KCl, 10 mM MgCl<sub>2</sub>, RNAs were analyzed on non-denaturing polyacrylamide gels in the presence of K<sup>+</sup> (20 mM) and Mg<sup>2+</sup> (5 mM) either (a) immediately after dilution, (c) after 12 h incubation at 20 °C, or (e) after heating to 90 °C for 3 min and snap-cooling on ice. Filled and empty squares represent the mean intensities of the dimer or monomer bands divided by the mean intensity of the entire lane, respectively. Monomer and dimer band assignments based on native electrophoretic and chromatographic analyses presented in ref. 1. Linear regression analyses of three independent experiments each (b, d, and f, respectively) indicate no increase in monomer band intensity with progressive dilution. Errors were propagated as the product of the mean times the square root of the sum of the squares of the individual variances divided by the individual means.



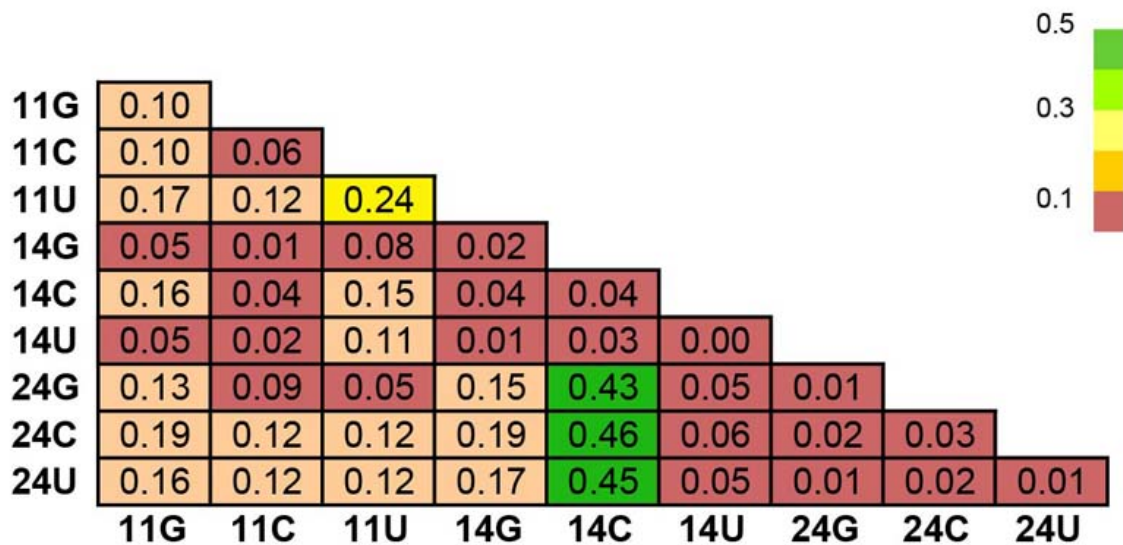
**Supplementary Figure 4** Structural features of the Corn-DFHO complex. **(a)** An extended ribose zipper-like interaction between nucleotides in J1, T4, T3 and T2. **(b)** A nine-tiered stack is formed by DFHO and purines from the core of the complex. The coaxial stack between DFHO, G12 and G25 extends in both directions, including nucleotides from T1, t1, T2, t2, T3 and t3. **(c)** The exocyclic amine of G8 forms a hydrogen bond with the carbonyl oxygen of G9.



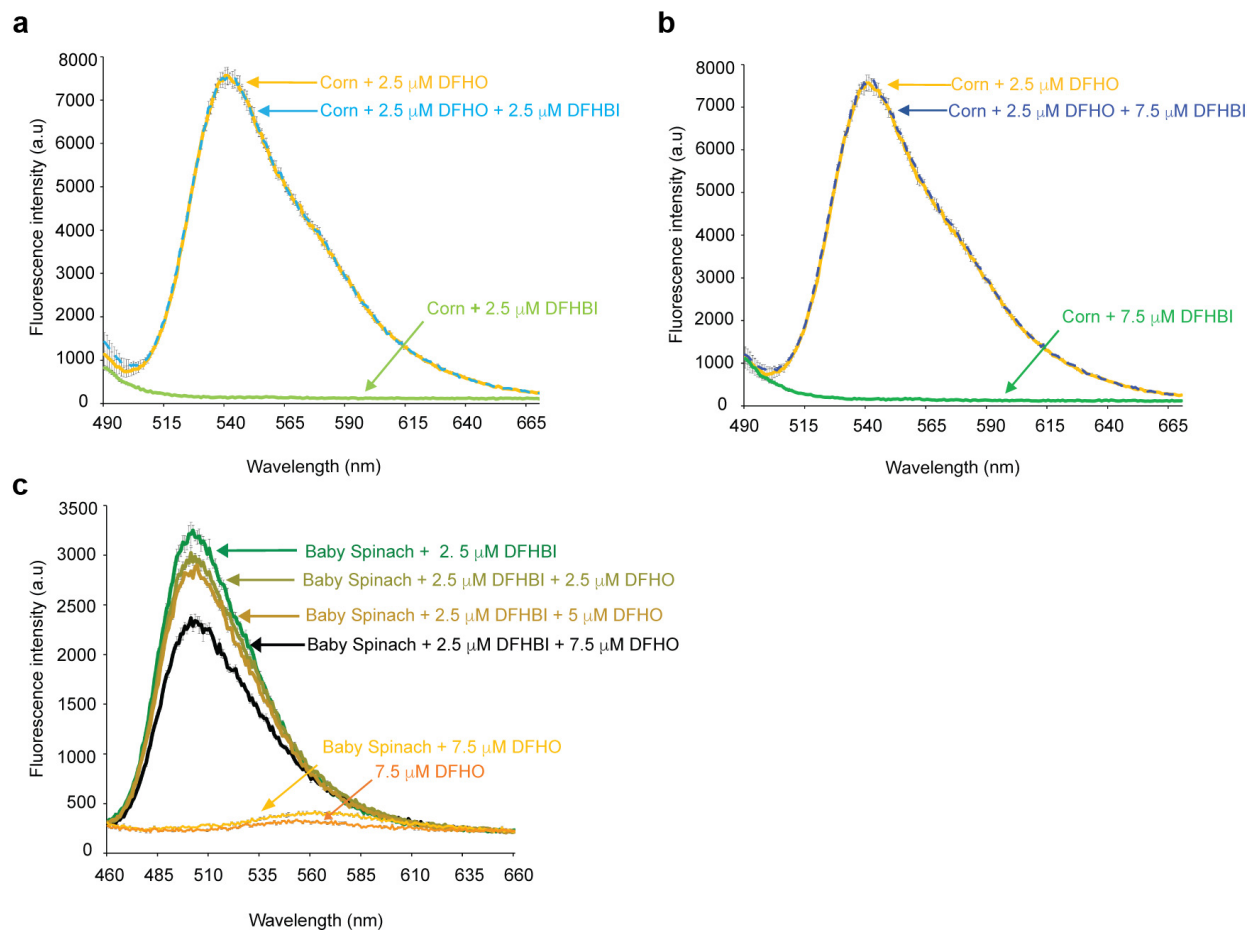
**Supplementary Figure 5** (a) Fluorescence lifetime of Corn-bound DFHO (red dashes). Gray dashes, DFHO in the absence of DFHO. Black dashes IRF, instrument response function. Yellow line, single exponential fit to the data. This fit, corrected for the IRF, gives a fluorescence lifetime of 4.31 ns. (b) Residuals from fit to a single exponential. Fluorescence intensity is in the same arbitrary units as in (a). (c) Residuals from fit to two exponentials. (d) Residuals from fit to three exponentials.



**Supplementary Figure 6** Fluorescence activation of thioflavin T (ThT) by Corn. **(a)** Fluorescence spectra of ThT in the presence and absence of Corn (yellow and red lines, respectively). Mean of three independent experiments and s.d. (black hashes) are shown. **(b)** Binding of ThT to Corn.  $K_d$  is approximately 3  $\mu\text{M}$ . Isotherm is the average of three independent experiments (error bars, s.d., depicted, but not visible at this scale). **(c)** Job plot of Corn-ThT association (error bars, s.d., depicted, but not visible at this scale).



**Supplementary Figure 7** Fluorescence activation by pairs of interfacial adenosine mutants of Corn. Error estimates are in **Supplementary Table 4**.



**Supplementary Figure 8** Corn and Spinach are orthogonal. **(a)** Fluorescence of 0.5  $\mu$ M Corn in the presence of excess DFHO, DFHO and DFHBI, and DFHBI. **(b)** As in **(a)** but in the presence of larger excesses of DFHBI. **(c)** Fluorescence of Baby Spinach (1  $\mu$ M) in the presence of DFHBI and excess DFHO. All spectra are means of three measurements. Black vertical lines, s.d.

## SUPPLEMENTARY REFERENCES

1. Song, W., Filonov, G.S. & Jaffrey, S.R. Imaging RNA polymerase III transcription dynamics using a photostable RNA-fluorophore complex. *Nature Chem Biol* (in press).